DOI 10.1007/s10812-020-01032-z
Journal of Applied Spectroscopy, Vol. 87, No. 3, July, 2020 (Russian Original Vol. 87, No. 3, May–June, 2020)

A RAMAN SPECTROSCOPIC STUDY OF THYMOQUINONE ANTITUMOR ACTION

A. V. Vcherashniaya,* I. V. Martinovich, G. G. Martinovich, O. I. Shadyro, and S. N. Cherenkevich

UDC 535.375.5; 543.424.2; 577.3'32/.'36

Fluorescence assay and Raman spectroscopy were used to study the mechanisms of action of 2-isopropyl-5-methyl-1,4-benzoquinone (thymoquinone) on HEp-2 human larynx carcinoma cells. Thymoquinone was found to have a more pronounced toxic effect than 1,4-benzoquinone and 2,3,5-trimethyl-1,4-benzoquinone. The action of thymoquinone leads to a decrease in the mitochondrial membrane potential and release of cytochrome c from the mitochondria, indicating activation of apoptosis of tumor cells through the mitochondrial-mediated pathway. These results indicate the possibility of using Raman spectroscopy in the study of programmed cell death.

Keywords: *Raman spectroscopy, apoptosis, thymoquinone, cancer cells.*

Introduction. The search for new regulators of programmed cell death and the detailed study of the mechanism of their action are high-priority areas of research in modern medical biophysics. Necrosis, apoptosis, and autophagy are among the major mechanisms for cell death [1]. Apoptosis and autophagy are physiologically programmed mechanisms for cell death, while necrosis is unregulated cell death upon the action of harmful factors [2–4]. Breakdown in the mechanisms for regulation of cell death is observed in many pathological processes including cancer. Thus, the search for effective inducers of programmed cell death and the development of new methods for studying molecular, biochemical, and biophysical indices permitting us to differentiate between various types of cell death are important steps in the development of modern biomedical technology.

Para-benzoquinones and their derivatives occupy a special place among the regulators of processes leading to the death of cancer cells. These compounds have antiviral and anti-inflammatory activity in addition to antitumor activity [5–7]. Thymoquinone (2-isopropyl-5-methyl-1,4-benzoquinone), found as a major component of the ethereal and nonvolatile oils of black caraway (*Nigella sativa*), is such a highly efficient bioregulator [7–9]. Reactive oxygen species (ROS) formed in cancer cells upon the action of thymoquinone are participants in redox signaling leading to the formation of mitochondrial permeability transition pores and the initiation of programmed cell death [10]. Since an increase in the production of ROS and the formation of mitochondrial permeability transition pores are observed in the signaling stages of autophagy and apoptosis, a detailed understanding of the mechanisms and differentiation of programmed cell death requires elucidation of the step involving initiation of the effector stage of the program (following signaling). Investigation of the subsequent stages of cell death is important for establishing the detailed mechanism of the action of thymoquinone. The protein cytochrome *c* is the most important participant in the activation of mitochondrial-mediated apoptosis. This protein acts as a trigger for the activation of the caspase cascade leading to the destruction of macromolecules and subsequent fragmentation of the cell into apoptotic bodies [11]. Thus, study of the processes involving distribution of cytochrome *c* will permit us to elucidate the initiation of apoptosis prior to the appearance of morphological changes in the cell.

Raman spectroscopy is now commonly used in studies of biological systems [12, 13]. In contrast to fluorescence methods requiring prior marking of the biomolecules or intracellular compartments by specific probes, Raman spectroscopy yields information about the local chemical composition of any part of the sample studied [14]. This noninvasive method has high spatial and time resolution, permitting observation and analysis of biochemical processes in living cells. Raman spectroscopy has been used to study the intracellular distribution of cytochrome *c* induced by the action of thymoquinone.

*To whom correspondence should be addressed.

Belorussian State University, 220030, Minsk, Belarus; email: vcherashniaya@gmail.com. Translated from Zhurnal Prikladnoi Spektroskopii, Vol. 87, No. 3, pp. 488–492, May–June, 2020. Original article submitted March 12, 2020.

Cytochrome *c* absorbs light with λ = 530 nm and a strong Raman spectrum can be observed due to the resonance absorption of exciting light with λ = 532 nm [15]. The Raman spectral band with maximum at 750 cm^{-1} is used to study the intracellular distribution of protein. This band is related to the vibrational mode of the pyrrole ring in the cytochrome c molecule [16, 17].

Materials and Methods. HEp-2 Human larynx epidermal carcinoma cells were used. The cells were cultured in DMEM medium from SigmaAldrich (USA) with added 8–10% embryonic bovine serum and 0.08 mg/mL gentamycin at 37°C in an atmosphere of 5% CO_2. The culture was carried out in sterile plastic flasks (25 cm^2 bottom) equipped with air filters. The cells were cultured in sterile plastic Petri dishes with diameter 35 mm to study the effect of *para*-benzoquinones (1,4-benzoquinone, 2-isopropyl-5-methyl-1,4-benzoquinone, and 2,3,5-trimethyl-1,4-benzoquinone) on proliferational activity. Upon reseeding, the cell concentration was $1 \cdot 10^{-5}$ cells/ml. The compounds were added to the Petri dish 24 h after reseeding of the cells. Cell counting was carried out 96 h after culturing.

A balanced buffer salt solution (BBSS) was used for the spectrooptical methods: 131 mM NaCl, 5 mM KCl, 1.3 mM $CaCl_2$, 1.3 mM $MgSO_4$, 0.4 mM KH_2PO_4, 20 mM HEPES, 6 mM glucose, pH 7.4.

For the studies using fluorescence analysis and Raman spectroscopy, the cell culture was carried out on silica plates in sterile Petri dishes. The cell concentration upon reseeding was $0.3 \cdot 10^5$ cells/mL. On the third day of the culture, the cell monolayer on the silica plate was washed twice with BBSS.

The Raman spectroscopic study of the intracellular distribution of cytochrome *c* was carried out using a spectroanalytical unit consisting of a LOTISTII Nanofinder HighEnd scanning confocal microscope (Belarus–Japan) and a 3.2-W laser with λ = 532 nm. The signal accumulation time was 2 s and the scan step was 1 mm.

The ethyl ester of tetramethylrhodamine (TMRE) has been used to measure the mitochondrial membrane potential. Cells in BBSS were incubated with 0.l-μM probe for 30 min at 37°C. The change in the mitochondrial membrane potential (ΔΨ) vs. elapsed time was measured using a Solar CM2203 spectrofluorimeter (manufactured in Belarus). The intensity of the TMRE fluorescence was measured at λ_{exc} = 545 nm and λ_{rec} = 590 nm. The protonophore carbonyl cyanide mchlorophenylhydrazone (CCCP) (5 μM) was used to determine the direction of change of the mitochondrial membrane potential. A study of the distribution of mitochondria in cancer cells and a qualitative evaluation of the change in the mitochondrial membrane potential were carried out using a spectro-analytical unit consisting of a LOTISTII Nanofinder HighEnd scanning confocal microscope (Belarus–Japan) and a 3.2 MW laser with λ = 532 nm (signal accumulation time 1 s and scan step 0.4 μm). The TMRE fluorescence was recorded at λ = 590 nm.

The kinetic curves presented are typical for a series of from three-to-five independent experiments. The results are given as mean values of the plus-minus standard deviation from the mean for from three-to-five independent experiments. The reliability was determined using Student's *t*-criterion at significance level $p < 0.05$ ($^*p < 0.05$ in comparison with the control).

Results and Discussion. A study was carried out on the effect of *para*-benzoquinones (1,4-benzoquinone, thymoquinone, and 2,3,5-trimethyl-1,4-benzoquinone) in concentrations 0.8–80 μM on the proliferative activity of HEp-2 human larynx carcinoma cells (Fig. 1). At such concentrations, these *para*benzoquinones cause a dosedependent decrease in the amount of cancer cells in the culture in comparison with the control sample. Thymoquinone proved to be the most toxic among the *para*-benzoquinones studied. The concentration for 50% inhibition (IC_{50}) of cell growth in the culture was 8 μM for thymoquinone, 25 μM for 1,4-benzoquinone, and 30 μM for 2,3,5-trimethyl-1,4-benzoquinone.

The change in the mitochondrial membrane potential was studied to establish the mechanisms of the toxic action of these *para*-benzoquinones. The addition of the *para*-benzoquinones to the indicated suspension of cancer cells led to a decrease in the TMRE fluorescence intensity, indicating a decrease in the mitochondrial membrane potential. Figure 2a gives curves for the dependence of the mitochondrial membrane potential of these cells on the concentration of thymoquinone and 2,3,5-trimethyl-1,4-benzoquinone. The decrease in the mitochondrial membrane potential becomes more pronounced with increasing concentration of the *para*-benzoquinones, especially for thymoquinone. The difference in the dependence of the decrease in the mitochondrial membrane potential on the concentration of the indicated compounds suggests a difference in the mechanisms of the their toxic action on cancer cells. Cyclosporin A, which is an inhibitor of the opening of mitochondrial permeability transition pores, was used to study the role of such pores in the quinone-induced decrease in the mitochondrial membrane potential. Cyclosporin A previously introduced into the cell suspension inhibited the decrease in the mitochondrial membrane potential by the action of thymoquinone (Fig. 2b). In contrast, the decrease in the mitochondrial membrane potential by the action of 1,4-benzoquinone and 2,3,5-trimethyl-1,4-benzoquinone was not blocked by cyclosporin A.

In order to elucidate the details of the mechanism of programmed cell death by the action of thymoquinone, a study was carried out on the intracellular distribution of cytochrome *c* before and after addition of this reagent. Figure 3a,b gives im-

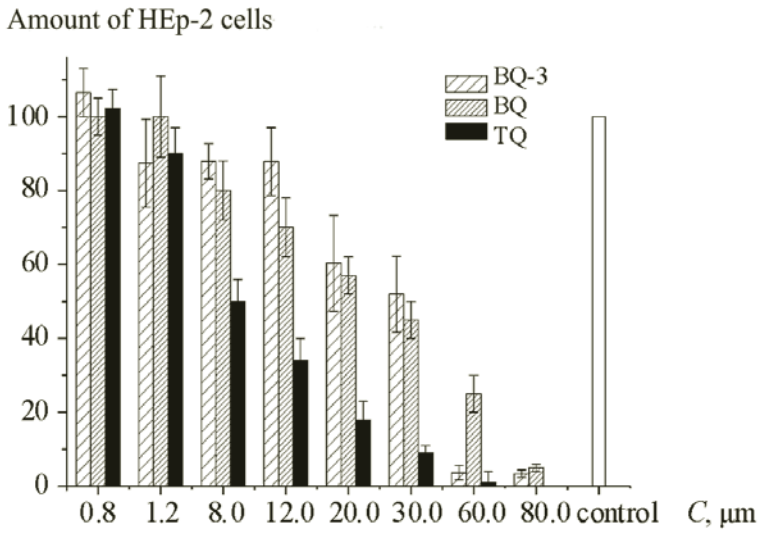

Fig. 1. Change in the amount of HEp-2 cells upon culture with *para*-benzoquinones: BQ3) 2,3,5-trimethyl-1,4-benzoquinone, BQ) 1,4-benzoquinone, and TQ) thymoquinone.

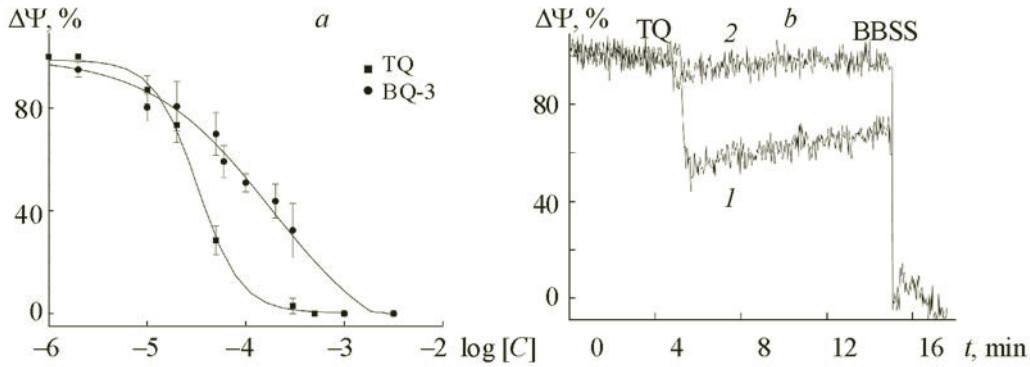

Fig. 2. Effect of *para*-benzoquinones on the mitochondrial membrane potential of HEp-2 cells: dependence of ΔΨ on the concentration of thymoquinone and 2,3,5-trimethyl-1,4-benzoquinone (a); effect of thymoquinone on ΔΨ: 20 μM thymoquinone (1) and 20 μM thymoquinone (cells incubated with cyclosporine A for 60 min) (2) (b).

ages of cancer cells converted relative to the intensity of the Raman spectral peak at 750 cm^{-1} characteristic for cytochrome c before and after the addition of thymoquinone. Figure 3c,d gives the corresponding curves for the intensity of this peak for cross section $y = 15$ μm. The intensity curves of the Raman spectral peak at 750 cm^{-1} show that prior to thymoquinone stimulation, intensity peaks are seen for regions in the vicinity of the cell membrane, indicating protein compartmentalization. Figure 3b shows that the addition of thymoquinone leads to intracellular redistribution of cytochrome *c*. In this case, the spectra of the thymoquinone-stimulated cells show a relatively homogeneous distribution of the intensity of the Raman spectral peak at 750 cm^{-1}, indicating the release of cytochrome *c* from the mitochondrial matrix into the cell cytosol (Fig. 3b,d).

A study of the role of mitochondria in the compartmentalization of cytochrome *c* was carried out using a laser confocal microscope and TMRE as a fluorescence probe. TMRE is a lipophilic cation with a delocalized charge, which is selectively accumulated in the most electronegative region of the cells, namely, the mitochondrial matrix. The amount of TMRE probe in the mitochondria depends on the potential on the inner mitochondrial membrane. Figure 4 gives fluorescent images of cancer cells colored by TMRE in the control and after the addition of thymoquinone. The predominant accumulation of the probe indicates localization of the mitochondria in the membrane regions of the control cells. The addition of thymoquinone leads to a decrease in the mitochondrial membrane potential accompanied by partial removal of the fluorescent probe from the mitochondria and a corresponding change in the intracellular distribution of the probe fluorescence intensity.

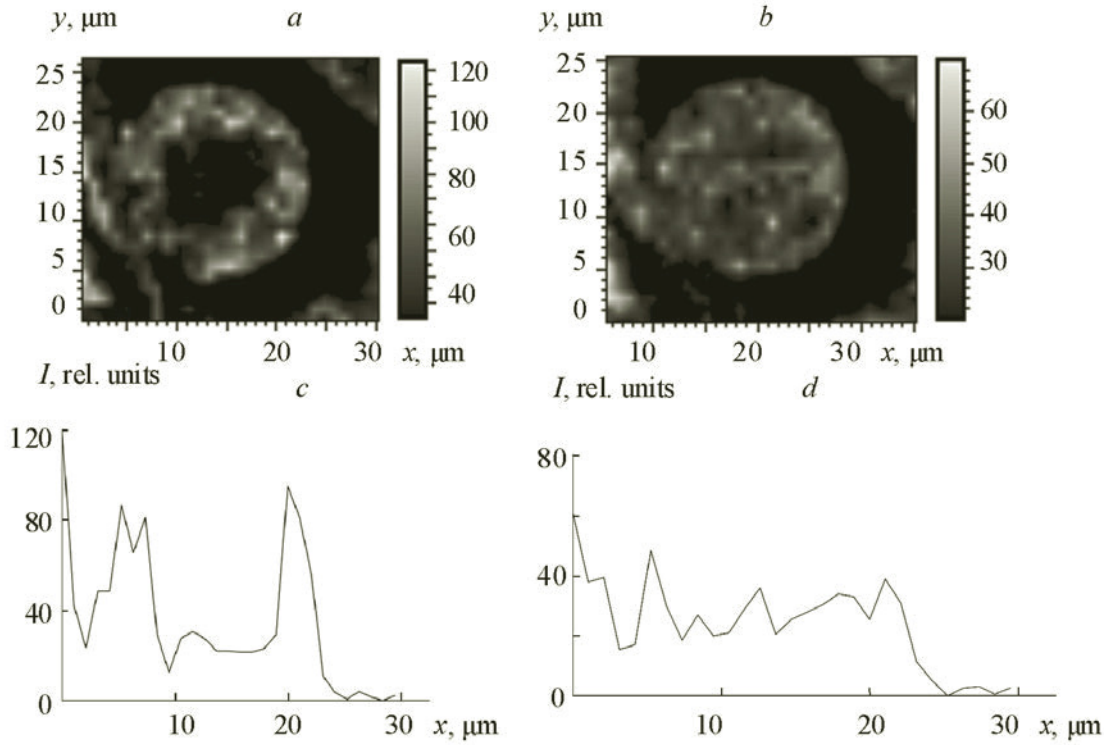

Fig. 3. Distribution of the intensity of the Raman spectral peak at 750 cm^{-1} in HEp-2 larynx carcinoma cells: control cells (a, c), cells in the presence of 20 μM thymoquinone (b, d).

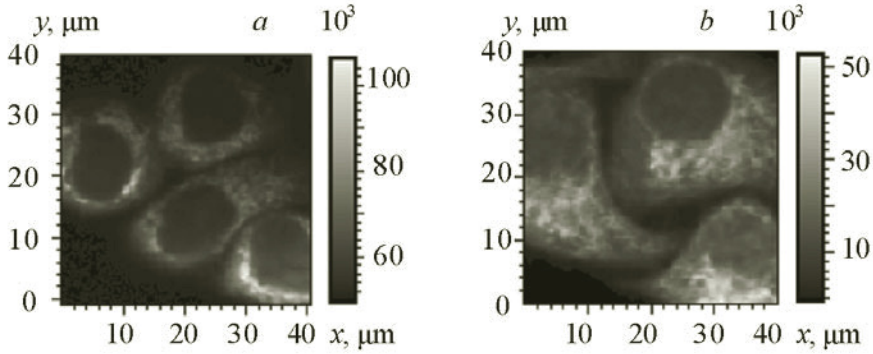

Fig. 4. TMRE fluorescence in HEp-2 human larynx carcinoma cells: a) control cells and b) with 20 μM thymoquinone.

The data obtained on the distribution of cytochrome *c* and the intracellular localization of the mitochondria indicate that thymoquinone induces programmed cell death of cancer cells through a mitochondrial-mediated pathway.

Conclusions. The data obtained using fluorescence analysis and Raman spectroscopy on the release of cytochrome *c* from the mitochondrial matrix upon the action of thymoquinone indicate activation of mitochondrial-mediated apoptosis in cancer cells. A Raman spectral study of the intracellular distribution of cytochrome *c* permitted us to follow the early stages of apoptosis, which is an important advantage of this method in comparison with biochemical and morphological methods for the study of programmed cell death.

REFERENCES

1. N. N. Daniel and S. J. Korsmeyer, *Cell*, **116**, 205–219 (2004).
2. J. Kerr, A. Willie, and A. Currie, *Brit. J. Cancer*, **26**, 239–257 (1972).
3. J. Doherty and E. H. Baehrecke, *Nat. Cell. Biol*., **20**, 1110–1117 (2018).
4. Q. Chen, J. Kang, and C. Fu, *Sig. Transduct. Target. Ther.*, **3**, No. 18, 1–11 (2018).
5. P. R. Dandawate, A. C. Vyas, S. B. Padhye, M. W. Singh, and J. B. Baruah, *Min. Rev. Med. Chem.*, **10**, No. 5, 436–454 (2010).
6. P. S. Shuveksh, K. Ahmed, S. Padhye, R. Schobert, and B. Biersack, *Curr. Med.*, **24**, No. 18, 1998–2009 (2017).
7. C. C. Wooa, A. P. Kumara, G. S. Kwong, and H. B. Tana, *Biochem. Pharmacol.*, **83**, No. 4, 443–451 (2012).
8. S. Banerjee, A. Padhye, A. Azmi, Z. Wang, P. A. Philip, O. Kucuk, F. H. Sarkar, and R. M. Mohammad, *Nutr. Cancer*., **62**, No. 7, 938–946 (2010).
9. R. Schneider-Stock, I. H. Fakhoury, A. M. Zaki, C. O. El-Baba, and H. U. Gali-Muhtasib, *Drug Discov. Today*, **19**, No. 1, 18–30 (2014).
10. G. G. Martinovich, I. V. Martinovich, A. V. Vcherashniaya, O. I. Shadyro, and S. N. Cherenkevich, *Biophys.*, **61**, No. 6, 963–970 (2016).
11. J. Cai, J. Yang, and D. P. Jones, *Biochim. Biophys. Acta*, **1366**, Nos. 1–2, 139–149 (1998).
12. H. Butler, L. Ashton, and B. Bird, *Nat. Protoc.*, **11**, 664–687 (2016).
13. R. Smith, K. L. Wright, and L. Ashton, *Analyst*, **141**, No. 12, 3590–3600 (2016).
14. K. Klein, A. M. Gigler, T. Aschenbrenner, R. Monetti, W. Bunk, F. Janitzkey, G. Morfill, R. W. Stark, and J. Schlegel, *Biophys. J.*, **102**, 360–368 (2012).
15. A. F. Palonpon, M. Sodeoka, and K. Fujita, *Curr. Opin. Chem. Biol.*, **17**, 708–715 (2013).
16. S. Hu, I. K. Morris, J. P. Singh, K. M. Smith, and T. G. Spiro, *J. Am. Chem. Soc.*, **115**, 12446–12458 (1993).
17. M. Okada, N. Smith, A. Palonpon, H. Endo, S. Kawata, M. Sodeoka, and K. Fujita, *Nat. Acad. Sci. USA*, **109**, 28–32 (2011).